

Understanding Focus Effects in Submicron Optical Lithography, Part 3: Methods for Depth-of-Focus Improvement

Chris A. Mack
FINLE Technologies, Plano, TX 75026

Abstract

In general, depth-of-focus (DOF) decreases as the square of the feature size. As the resolution of optical lithography has improved, with the potential to go below $0.25\ \mu\text{m}$, the decrease in usable DOF has been significant. As such, there has been increasing effort put towards ways of improving DOF in manufacturing. This paper will examine several proposed techniques for improving DOF including the use of geometry dependent mask bias, variable numerical aperture, multiple focal-plane exposures (the FLEX method), frequency plane spatial filtering, and annular illumination sources. As will be shown, each method offers the potential for improved DOF, but only for certain cases. None of the methods provides a general solution to the problem of shrinking focal depth, but rather they may simply slow the inevitable progression.

I. Introduction

Depth-of-focus (DOF) continues to be one of the most critical process latitudes in optical lithography. As features continue to shrink, focus latitude shrinks as well. However, focus errors are difficult to reduce and in many production environments the "resolution" is in fact determined by DOF considerations. This paper will review several proposed methods for improving DOF, but first a review of basic focus effects is in order.

The term DOF is often used as a catch all for any focus effect in optical lithography. It is important to realize, however, that there are two distinct aspects of focus issues in manufacturing: process requirements and process capabilities. A particular process *requires* a minimum depth-of-focus due to numerous built in focus errors of the process. For example, topography is a constant for a given layer and results in a direct focus error (the top and bottom of the topography cannot both be in focus). Built in focus errors (BIFE) can be either random (e.g., vibration) or systematic (e.g., topography). A careful analysis of the sources of BIFE is essential in order to determine a process focus requirement. Table I shows the results of a hypothetical analysis of a typical $0.5\ \mu\text{m}$ process with a 4X reduction stepper. Note that the

random errors are first added RMS and then added to the systematic errors. It is apparent from such an analysis which errors cause the greatest problems (in this case wafer non-flatness, best focus determination, topography, and field curvature and astigmatism).

Table I - Example of Focus Process Requirement Analysis

Estimated Built In Focus Errors (BIFE)	Total Range (μm)
Random Errors:	
Lens Heating (compensated)	0.10
Environmental (compensated)	0.20
Mask Tilt ($0.7 \mu\text{m} / 16$)	0.05
Mask Flatness ($2.0 \mu\text{m} / 16$)	0.12
Wafer Flatness (25 mm field)	0.50
Chuck Flatness (25 mm field)	0.14
Autofocus Repeatability	0.20
Best Focus Determination	0.40
Vibration	0.10
Total RMS Random Focus Errors:	0.74
Topography	0.5
Field Curvature and Astigmatism	0.4
Resist Thickness	0.2
Total BIFE (range)	1.8 μm

Independent of process requirements, *process capability* describes how a lithographic process responds to focus errors. Depth-of-focus is actually a term which describes process capability, but it is so poorly defined that it can mean virtually anything depending on how it is used. A less-abused term is focus latitude which, like any latitude, is defined as the response of the process to a given error. If the process capability exceeds the process requirements then reasonable manufacturing yields can be obtained. Since the ultimate goal is yield, the lithographer can either reduce the process requirements (by reducing the BIFE) or increase the process capability (by increasing the DOF) to achieve improved yield. Any successful strategy for scaling a process to smaller dimensions must encompass both of these approaches.

Defining focus latitude is complicated by its extreme dependence on exposure energy, just as exposure latitude is dependent on focus. Thus, a definition of DOF is only useful if it describes the coupled exposure-focus dependency. The best description of DOF comes from the focus-exposure process window. For a given process specification, the focus-exposure process window is a plot of all those values of focus and exposure which keep the process within specification. The most common specifications are linewidth and resist sidewall angle, but resist loss can also be used. Measuring the process window, however, can be time consuming and

difficult. Thus, simpler metrics for DOF are often used. When analyzing aerial images, the log-slope defocus curve is useful [1-3], in which the slope of the logarithm of the aerial image at the line edge is plotted versus defocus. When comparing images for different feature sizes the normalized log-slope should be used, which is just the image log-slope times the nominal linewidth. The log-slope is directly related to exposure latitude [4], so the log-slope defocus curve describes, in a simple fashion, how exposure latitude falls off with defocus.

The following sections describe a variety of techniques which have been proposed to improve the depth-of-focus for high resolution lithography processes. Some techniques are quite old (properly biasing the mask), but still have not found widespread use. Some techniques are old to optics but new to lithography (spatial filtering, phase-shifting masks) and still unproven. The goal here will be to give some indication of the benefits and detriments of each method.

II. Mask Bias

Originally, adding bias to a mask was used as a means of compensating for subsequent process steps which changed the dimensions of the final structure from that defined in the lithographic step. With the advent of high resolution positive resists it became known that process latitude could be improved by overexposing. Thus, by oversizing the chrome features on the mask and overexposing the resist correct linewidths could be obtained with improved latitude. The drawback, of course, was throughput. There are two main reasons why this type of biasing works: 1) improvement of the latent image through higher exposures [4] and 2) improvement of the image log-slope [5].

The simplest way to bias a mask is to apply the same bias to all features. However, not all features need the same bias. In fact, the simplicity of a uniform bias is the main reason why bias is not used to its full potential. For each feature there is an optimum bias which maximizes the size of its process window. Further, the optimum bias varies considerably with feature size and type [5]. For example, isolated lines benefit greatly from a relatively large amount of bias, but high resolution line/space arrays do not. Figure 1a shows the improvement of the normalized image log-slope with bias (to a point) for several sizes of isolated lines with $0.75\mu\text{m}$ of defocus as calculated by the lithography simulator PROLITH/2 (FINLE Technologies, Plano, TX). Figure 1b shows that dense arrays of lines and spaces do not show this improvement for the smallest and largest line sizes. What is needed is a geometry dependent bias. Implemented as a CAD algorithm, geometry dependent bias would examine the feature size and type and the proximity of other features to determine the amount of bias based on the following two criterion. First, the critical feature(s) would be biased to improve performance. Next, the rest of the mask would be biased to print properly at the energy needed to print the critical feature(s). Although significantly more complicated than a uniform bias, an algorithm of this type is certainly within our capabilities. Yet, only recently have attempts to define such an algorithm for limited

structures been published [6]. It is interesting to note that such an algorithm is a subset of the problem which must be solved in order to design optimized phase-shifting masks. Thus, industry focus on the problem of geometry dependent bias would find immediate benefit and serve as an important first step in the automated design of phase-shifting masks.

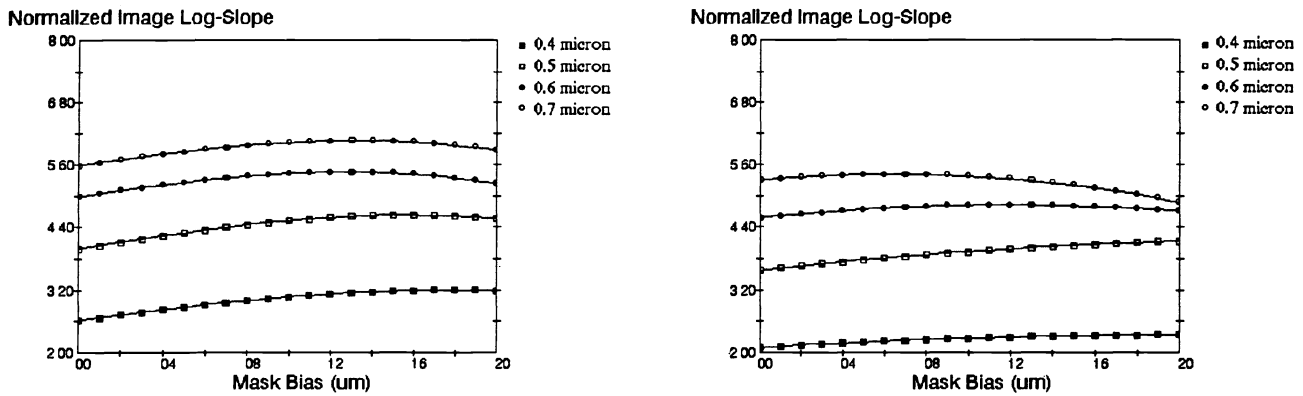


Figure 1. The effect of mask bias on the normalized image log-slope for (a) isolated lines, and (b) line/spaces arrays of various nominal linewidths with a defocus of $0.75\mu\text{m}$ (calculated with PROLITH/2).

III. Variable Numerical Aperture and Partial Coherence

In 1989 the author introduced the concept of "image manipulation," varying the numerical aperture (NA) and partial coherence (σ) of a stepper on a level by level basis in order to optimize the shape of the aerial image for the critical feature(s) on each level [7,8]. The effect of numerical aperture on DOF is not obvious and is strongly dependent on the feature size and type as well as the partial coherence. Using the image log-slope as a means of judging image quality, Figure 2a shows that numerical aperture significantly affects the shape of the log-slope defocus curve. In focus, the higher numerical apertures result in higher log-slopes, and thus improved imaging. However, when there is defocus, higher NA may result in decreased log-slope (i.e., at some value of defocus the log-slope curves for two different numerical apertures will cross). One way to interpret this result is that for a given amount of defocus, there is one value of the numerical aperture which gives the maximum log-slope of the aerial image. As shown in Figure 2b, this optimum NA is also a function of feature type. For a given feature type and size and a given amount of defocus, there is one NA which gives optimum image quality. Likewise, for a given feature type and size and a minimum acceptable image quality (i.e., minimum value of the log-slope) there is one NA which will give the maximum DOF.

The partial coherence can also greatly affect the optimum NA. If a projection tool has a variable objective lens numerical aperture, by default it must also have a variable condenser lens

numerical aperture for σ to remain constant. Thus, σ could also be varied in such a system. Consider the imaging of $0.45\mu\text{m}$ lines and spaces with i-line assuming $0.75\mu\text{m}$ of defocus is expected in the process (i.e., the BIFE). By varying both the numerical aperture and the partial coherence, contour plots of constant image log-slope can be generated, as shown in Figure 3. In this case, the optimum log-slope occurs when $\text{NA} = 0.45$ and $\sigma = 0.10$ (where a value of 0.1 was the lowest examined). For $0.4\mu\text{m}$ lines and spaces, however, the optimum NA is 0.55 with σ equal to 0.65.

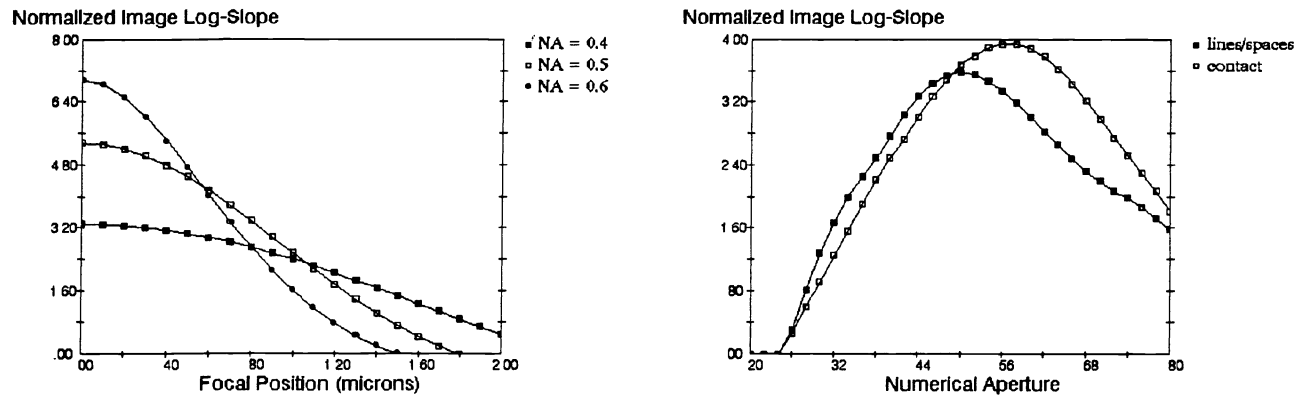


Figure 2. Finding the optimum numerical aperture using the image log-slope as a metric. (a) The log-slope defocus curves cross indicating the one NA is better than another only over a certain focus range. (b) For $0.75\mu\text{m}$ defocus, the optimum NA for an array of lines and spaces is 0.5, but for an array of contacts it is 0.57 ($\sigma = 0.5$, i-line, $0.5\mu\text{m}$ features, as calculated by PROLITH/2).

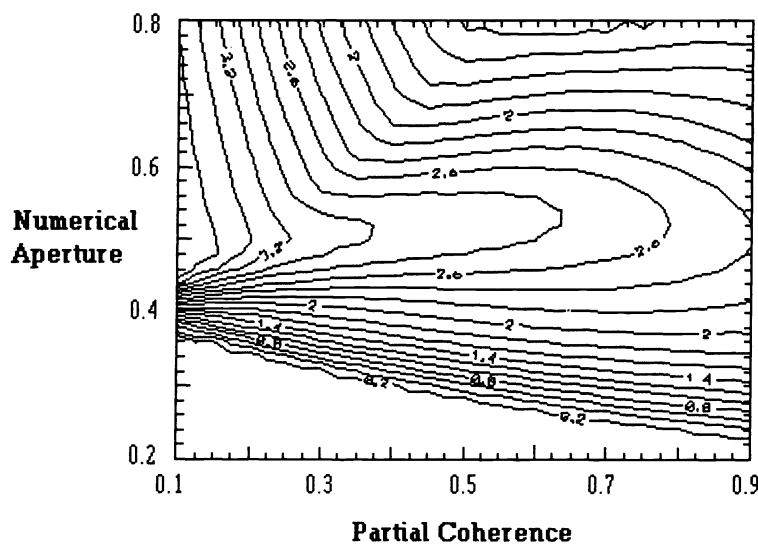


Figure 3. Contour map of image-log slope as a function of the numerical aperture and partial coherence of the projection system ($0.45\mu\text{m}$ lines and spaces, i-line, $0.75\mu\text{m}$ defocus).

Although a very useful indicator, it is not possible to determine the true optimum values of NA and σ based solely on log-slope. Another approach is to use the Lumped Parameter Model (LPM) to predict the size of the process window [9]. The LPM is a simple model for resist exposure and development that allows for the calculation of an entire focus-exposure matrix on a PC in matter of seconds. Though certainly not as accurate as the primary parameter models found in programs such as PROLITH/2 and SAMPLE, the LPM is more accurate than any metric based solely on aerial images (e.g., the image log-slope). Using an optimization routine built into PROLITH/2, numerical aperture and partial coherence can be varied in order to maximize the size of the focus-exposure process window (as predicted by the LPM over a specified focus range). Based on this approach, the case of $0.45\mu\text{m}$ lines and spaces discussed above has an optimum LPM process window when $\text{NA} = 0.49$ and $\sigma = 0.22$. Both the log-slope and LPM approaches can be used to quickly determine the approximate optimum stepper settings, which can then be investigated further with the more exact primary parameter models and finally experimental data.

IV. Multiple Focal Plane Exposures

Recently, Fukuda and coworkers from Hitachi introduced a method, which they called FLEX [10-12], with the potential to improve depth-of-focus. In its simplest form, a wafer would be given a partial exposure at a particular focal position. Then, without moving the wafer in the x or y directions, the wafer would be moved to a different focal position and the remaining exposure would be delivered. The result is an averaging of aerial images both in and out of focus. Although two focal plane exposures are a minimum, more focal planes can be used. Typically, only two or three planes have been used since more exposures tend to add complexity without giving further benefit. Besides processing complexity and decreased throughput, what are the trade-offs of using this technique? How much benefit can be expected? To answer these questions, the lithography simulator PROLITH/2 was enhanced to include multiple focal plane exposures.

The log-slope defocus curve will again be a useful technique for understanding the effects on DOF. For a multiple focal plane exposure, the final aerial image can be thought of as a summation of the aerial images at the different focal planes, weighted by their respective exposure energies. For the cases studied here, three focal planes will be used separated from each other by a distance ΔF , all with equal exposures. Once an "average" aerial image is computed, its log-slope can also be determined. Figure 4a shows the effect of ΔF on the log-slope defocus response for $0.5\mu\text{m}$ lines and spaces ($\text{NA} = 0.5$, $\sigma = 0.5$, i-line). A $\Delta F = 0$ indicates the standard single focal plane exposure. Some statements can be made about this graph which I have found to be generally true for multiple focal plane exposures: (1) this technique results in improved log-slope for out-of-focus conditions, but only at the expense of reduced performance in focus; and (2) the focus value at which the curves cross (in this case both are at $1.2\mu\text{m}$ of defocus) is beyond what would normally be considered the depth-of-focus

of the system. Further, for the case of equal lines and spaces, the crossover point occurs at an extremely low value of the log-slope, making the use of FLEX for lines and spaces undesirable.

Figure 4b shows the same simulations for the case of an array of $0.5\mu\text{m}$ contacts. The basic trends are the same but now the crossover point occurs at a much more reasonable, though still low, value of the normalized log-slope. Although the log-slope defocus curve gives a great amount of insight into the behavior or multiple focal plane exposures, it does not tell the full story. In particular, the log-slope defocus curve gives no information about isofocal bias. Figure 5a shows a focus-exposure process window for a $0.5\mu\text{m}$ contact with a standard single pass exposure. Values of focus and exposure which are within this window have linewidths which are within $\pm 10\%$ of the nominal value. A limiting feature of this window is its curvature. As the contact goes out of focus, more energy is required to properly size it. Thus, the curvature of the window is indicative of an extreme isofocal bias which will significantly limit the overall depth-of-focus. The log-slope defocus curve gives no indication that this isofocal bias exists (and, in fact, it does not exist to any great extent for the case of equal lines and spaces). Examining the process window resulting from a three-pass multiple focal plane exposure with $\Delta F = 1.5\mu\text{m}$, one can see that the isofocal bias has essentially been eliminated. Although the size of the window in focus has diminished (i.e., there is less exposure latitude in focus), the window stays essentially the same size over a long focus range. Thus, if the smaller exposure latitude is acceptable, the DOF of these contacts can be improved using FLEX.

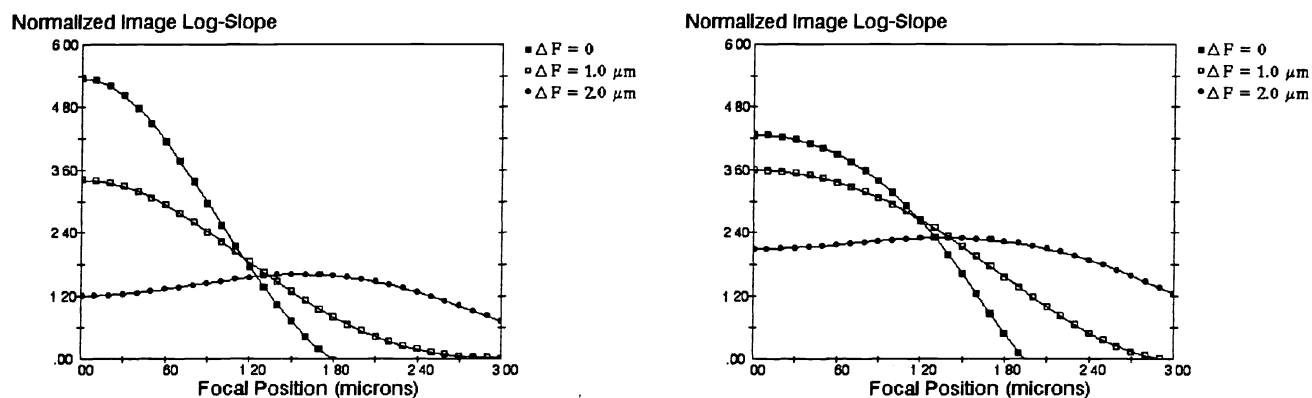


Figure 4. The effect of multiple focal plane exposures on the log-slope defocus curve for (a) equal lines and spaces and (b) contacts ($0.5\mu\text{m}$ features, $\text{NA} = 0.5$, $\sigma = 0.5$, i-line, three-pass exposures with separation between focal planes of ΔF).

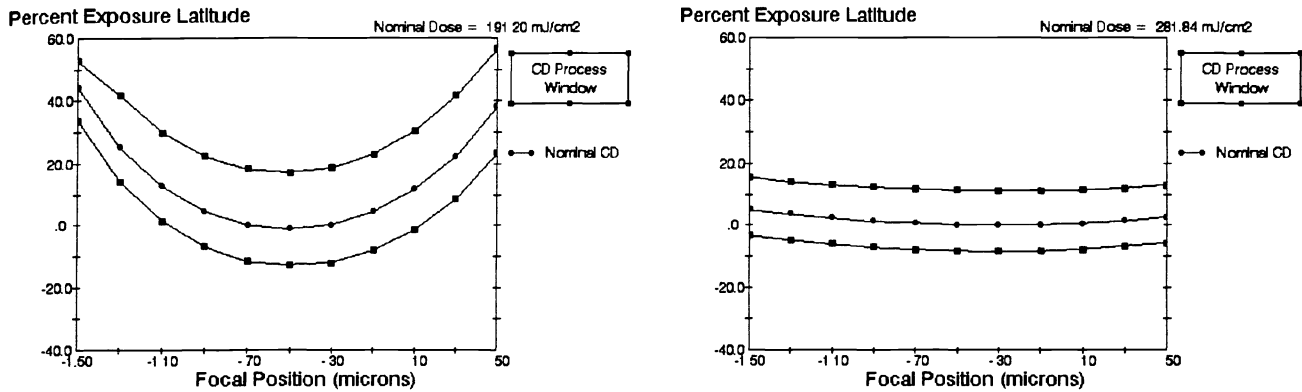


Figure 5. The effect of multiple focal plane exposures on the shape of the focus-exposure process window: (a) no FLEX and (b) three-pass exposures with a focal plane separation of $1.5\mu\text{m}$ ($0.5\mu\text{m}$ contacts, $\text{NA} = 0.5$, $\sigma = 0.5$, i-line).

Figure 5 shows that the main benefit of the FLEX method for contacts is to reduce, and even eliminate, the isofocal bias. In fact, the optimum focal plane separation can be found as the value which completely eliminates the isofocal bias (in this case, this value is slightly greater than $1.5\mu\text{m}$). The price that must be paid is a reduction in exposure latitude and photoresist sidewall angle when in focus. The unique imaging attributes of contacts in positive photoresist (i.e., a strong isofocal bias) make the FLEX method particularly appropriate, whereas other types of features do not see much benefit.

V. Spatial Frequency Filtering

The concept of spatial frequency filtering is not a new one. The earliest filter to be studied was the simple annular aperture in which the central portion of the objective lens pupil is blocked. The use of an annular aperture was first suggested by Lord Rayleigh as a means of improving resolution [13], though it had been studied mathematically much earlier. Steward [14] studied this aperture and found that it gave "...a decided gain in resolving power..." at the expense of throughput due to the loss of light. Welford [15] later studied annular apertures and found that they also improved depth-of-focus, but produced secondary image maxima of greater intensity (commonly called side-lobes today). Welford also suggested that proper adjustment of the response of the photographic media could reduce the printability of these side-lobes, as has been recently suggested for photoresists [16]. Jacquinot et al. [17] described an application in which the outer portions of the aperture were reduced in transmission and coined the term *apodization* to describe this filtering technique. Although the result of this filter is reduced resolution, the use of the term apodization has grown to encompass any modification of the transmission properties, real or complex, of a lens pupil (for an early review of work in this area, see ref. [18]). Duffieux is given credit for introducing Fourier frequency analysis to optics in his

1946 book, which has only recently been translated into English [19]. Thus, modification of the transmission function of a lens aperture has come to be known as spatial frequency filtering (see Goodman's classic textbook for a review of spatial filtering [20]). In fact, the effect of a central aperture stop on the frequency response of an imaging system is given as a homework problem by Goodman (Chapter 6, problem 6-1).

Recently, spatial filtering has been proposed for microlithography [21,22]. The proposed filters has been similar in principle to an annular aperture, but rather than having a transmission of zero in the central portion of the aperture the transmission is simply reduced. For example, a filter, which could be located at either the entrance pupil or the exit pupil of the objective lens, may have a transmission of 50% out to a radius of one-half of the pupil radius, with 100% transmission for the outer half of the pupil. Although a pure transmission filter would be much simpler to fabricate, shifters could be added as well. Thus, for example, our simple filter could be modified to have 50% transmission *and* a 180° phase shift in the central portion of the aperture. In general, a radially symmetric filter can be described by its complex transmission function $\tau(r)$ where r is the radial position within the pupil relative to the pupil diameter.

As an example of the effect of a simple filter on a simple aerial image, consider the coherent image of a $0.5\mu\text{m}$ line/space array such that only the zero and first diffraction orders make it through the lens. The resulting aerial image intensity is given by

$$I(x) = \left[\frac{1}{2} + \frac{2}{\pi} \cos(2\pi x/p) \right] \quad (1)$$

where the cosine term results from the first diffraction orders and the one-half term results from the zero order. Consider now our simple filter where the central portion of light in the aperture is attenuated by passing through a filter with electric field transmission T . Further, let us pick the radius of this central region to be such that the zero order is attenuated but the first order is not. Thus, the filtered aerial image is

$$I(x) = \left[\frac{1}{2} T + \frac{2}{\pi} \cos(2\pi x/p) \right] \quad (2)$$

It is a simple matter to plot equation (2) and determine the effect of various transmissions on the image, as shown in Figure 6, where each image was normalized to have the same peak intensity for comparison purposes. The effects are as expected. The edge slope of the space increases as the transmission is reduced, but at the expense of increased side lobe intensity. In fact, if $T=0$, the result is a dark field frequency doubled image [23].

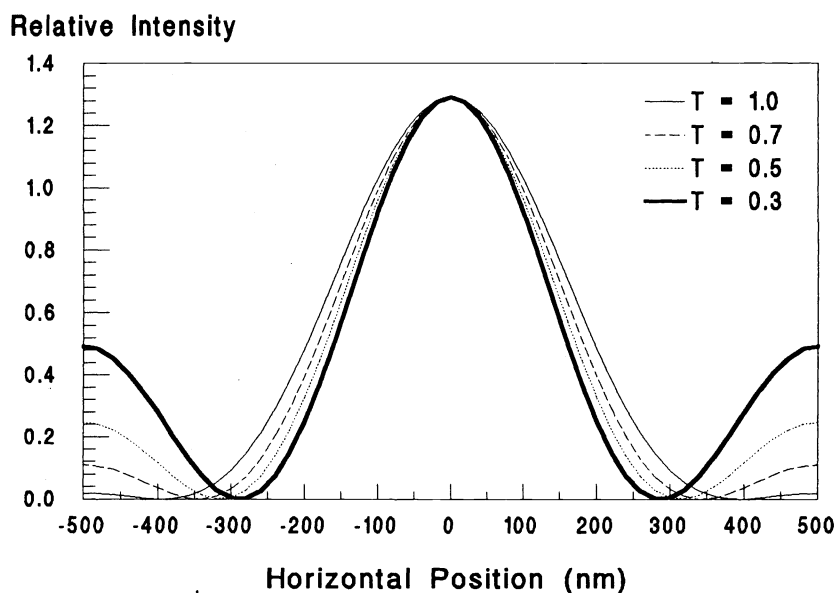


Figure 6. Effect of spatial filtering on an image of equal lines and spaces with coherent illumination for a simple filter which reduces the amplitude of the zero order by T . Images are normalized to have the same peak intensity for comparison purposes.

Of course, more complicated filters will have different responses, but the general trends will be similar. Several notes of caution are in order. For any given filter, the effect on the aerial image will be different for different feature sizes and types. Thus, in general, the first casualties of spatial frequency filtering are mask linearity and the proximity effect. These issues must be looked at very closely when designing a filter. A filter design can be fully optimized only for a particular feature. Thus, to get the most out of such a filter arrangement the filters must be easily interchangeable so that different mask levels can each be optimized. In light of these issues, it would be highly desirable to have only one critical feature per mask level when using spatial filtering.

VI. Annular and Other Illumination Sources

Variations of the method of illumination seem to have received very little attention over the years as a means of improving imaging. Recently, both theoretical [7] and experimental [24] studies have shown the potential for improving image quality with annular illumination systems. Further work included the combination of annular illumination with a centrally obscured objective lens pupil [25]. Very recently, the use of various illumination shapes has generated considerable interest and the most recent studies are in these proceedings [26,27].

The effect of annular illumination can be summed up quite nicely by examining the variation of the aerial image log-slope with linewidth. Figure 7 compares this variation for both conventional and annular illumination systems. As can be seen, the annular source results in

improved image quality for certain small features (in this case for features near $0.3\mu\text{m}$) at the expense of reduced image quality for larger features ($0.4 - 0.7\mu\text{m}$ here). This is the essential trade-off for any illumination modification. If the response of one feature size is improved, other features will suffer. Thus, as before, there is an advantage to using various illuminator shapes, but only if they are easily changeable and if there are very few (preferably one) critical features per mask level.

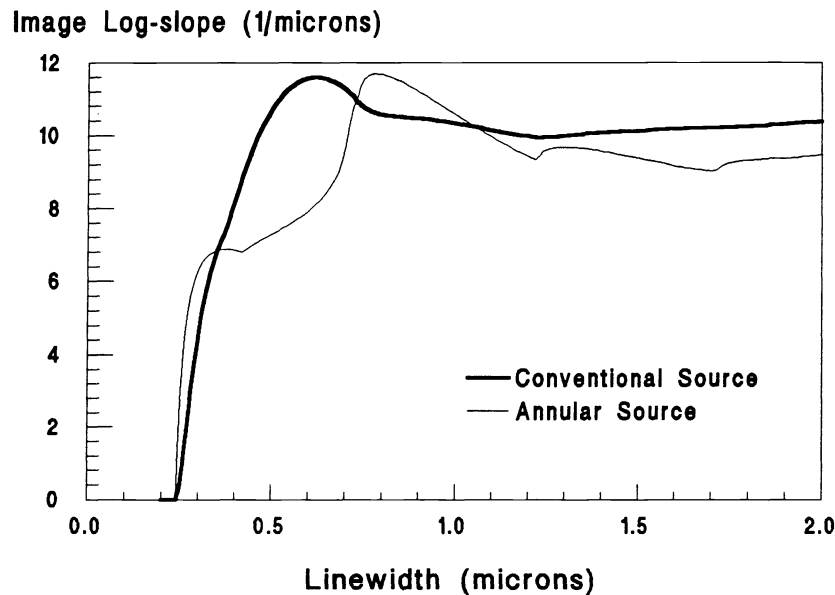


Figure 7. Comparison of conventional and annular sources for line/space pairs of varying width (NA = 0.5, i-line, no defocus, $\sigma = 0.5$ for the conventional source, and the annular source is a very thin annulus about $\sigma = 0.5$).

VII. Conclusions

All of the methods for DOF improvement reviewed here have some merit. In general, depth-of-focus for one feature can be improved at the expense of other features. Usually mask linearity and proximity effects suffer, but they should be carefully examined in any case. One proposed method, geometry dependent mask bias, would by design alleviate linearity and proximity type effects. Although not discussed here, phase-shifting masks also represent an opportunity for DOF improvement, with many of the same problems. There is, however, one technique for improving lithographic performance in the face of shrinking depth-of-focus which has none of these negative side effects: reducing the built in focus errors. Obviously lens designers and manufacturers are actively working on reducing lens induced focus errors and the need for ultra-flat wafers is well known. Planarization techniques are also receiving considerable attention. One area that could use further work is best focus determination and new techniques such as latent image metrology hold great promise.

References

1. H. J. Levenson and W. H. Arnold, "Focus: The Critical Parameter for Submicron Lithography," *Journal Vacuum Science and Tech.*, Vol. B5 (Jan/Feb 1987) pp. 293-298.
2. C. A. Mack, "Understanding Focus Effects in Submicron Optical Lithography," *Optical/Laser Microlith., Proc.*, SPIE Vol. 922 (1988) pp. 135-148, and *Optical Engineering*, Vol. 27, No. 12 (Dec. 1988) pp. 1093-1100.
3. C. A. Mack and P. M. Kaufman, "Understanding Focus Effects in Submicron Optical Lithography, Part 2: Photoresist Effects" *Optical/Laser Microlith. II, Proc.*, SPIE Vol. 1088 (1989) pp. 304-323.
4. C. A. Mack, "Photoresist Process Optimization," *KTI Microelectronics Seminar, Proc.*, (1987) pp. 153-167.
5. C. A. Mack and P. M. Kaufman, "Mask Bias in Submicron Optical Lithography," *Journal of Vacuum Science and Technology*, Vol. B6, No. 6 (Nov./Dec. 1988) pp. 2213-2220.
6. N. Shamma, F. Sporon-Fielder and E. Lin, "A Method for Correction of Proximity Effect in Optical Projection Lithography," *KTI Microelectronics Seminar, Proc.*, (1991) pp. 145-156.
7. C. A. Mack, "Optimum Stepper Performance Through Image Manipulation," *KTI Microelectronics Seminar, Proc.*, (1989) pp. 209-215.
8. C. A. Mack, "An Algorithm for Optimizing Stepper Performance Through Image Manipulation," *Optical/Laser Microlithography III, Proc.*, SPIE Vol. 1264 (1990) pp. 71-82.
9. C. A. Mack, A. Stephanakis, R. Hershel, "Lumped Parameter Model of the Photolithographic Process," *Kodak Microelectronics Seminar, Proc.*, (1986) pp. 228-238.
10. H. Fukuda, N. Hasegawa, T. Tanaka, and T. Hayashida, "A New Method for Enhancing Focus Latitude in Optical Lithography: FLEX," *IEEE Electron Devices Letters*, Vol. EDL-8, No. 4 (Apr 87) pp. 179-180.
11. T. Hayashida, H. Fukuda, T. Tanaka, and N. Hasegawa, "A Novel Method for Improving the Defocus Tolerance in Step and Repeat Photolithography," *Optical Microlithography VI, Proc.*, SPIE Vol. 772 (1987) pp. 66-71.
12. H. Fukuda, et al., "Method for Forming Pattern and Projection Aligner for Carrying Out Same," U.S. Patent 4,869,999 (issued Sep 89).
13. Lord Rayleigh, "On the Diffraction of Object Glasses," *Astronomical Society Monthly Notice*, Vol. 33 (1872) pp. 59-63, also reprinted in his book *Scientific Papers Vol. I*, Dover Publications (New York: 1964) pp. 163-166.

14. G. C. Steward, The Symmetrical Optical System, Cambridge University Press (London: 1928) pp. 88-94.
15. W. T. Welford, "Use of Annular Apertures to Increase Focal Depth," *Journal of the Optical Society of America*, Vol. 50, No. 8 (Aug 1960) pp. 749-753.
16. P. M. Spragg, et al., "Optimization of Positive Novolak-Based Resists for Phase Shift Mask Technology," *Optical/Laser Microlithography V, Proc.*, SPIE Vol. 1674 (1992, to be published in this proceedings).
17. P. Jacquinot, et al., *Comptes Rendus de L'Academie des Science, Paris*, Vol. 223 (1946) pp. 641 (in french).
18. E. Wolf, "The Diffraction Theory of Aberrations," *Reports on Progress in Physics*, Vol. 14 (1951) pp. 109-111.
19. P. M. Duffieux, The Fourier Transform and Its Application to Optics, John Wiley & Sons (New York: 1983).
20. J. W. Goodman, Introduction to Fourier Optics, McGraw-Hill (New York: 1968).
21. H. Fukuda, T. Terasawa, and S. Okazaki, "Spatial Filtering for Depth of Focus and Resolution Enhancement in Optical Lithography," *Journal of Vacuum Science and Technology*, Vol. B9, No. 6 (Nov/Dec 1991) pp. 3113-3116.
22. W. Henke and U. Glaubitz, "Increasing Resolution and Depth of Focus in Optical Microlithography through Spatial Filtering Techniques," *Microcircuit Engineering '91* (to be published).
23. C.A. Mack, "Fundamental Issues in Phase-Shifting Mask Technology," *KTI Microlithography Seminar, Proc.*, (1991) pp. 23-35.
24. D. L. Fehrs, H. B. Lovering, and R. T. Scruton, "Illuminator Modification of an Optical Aligner," *KTI Microelectronics Seminar, Proc.*, (1989) pp. 216-230.
25. S. T. Yang, et al., "Effect of Central Obscuration on Image Formation in Projection Lithography," *Optical/Laser Microlithography III, Proc.*, SPIE Vol. 1264 (1990) pp. 477-485.
26. N. Shiraishi, et al., "New Imaging Technique for 64M-DRAM," *Optical/Laser Microlithography V, Proc.*, SPIE Vol. 1674 (1992, to be published in this proceedings).
27. K. Tounai, H. Tanabe, H. Nozue, and K. Kasama, "Resolution Improvement with Annular Illumination," *Optical/Laser Microlithography V, Proc.*, SPIE Vol. 1674 (1992, to be published in this proceedings).